1 **Low sedimentary accumulation of lead caused by weak downward export of organic matter**

2 **in Hudson Bay, northern Canada**

3

4

5 Benoit Thibodeau[1,2], Christophe Migon[3], Aurélie Dufour[3], André Poirier[4], Xavier Mari[3,5],
6 Bassam Ghaleb[4] and Louis Legendre[3]

7

8

9

10

11 [1]Department of Earth Sciences, The University of Hong Kong, Pokfulam Road, Hong Kong

12 [2]Swire Institute for Marine Science, The University of Hong Kong, Cape d'Aguilar Road, Shek
13 O, Hong Kong SAR

14 [3]Sorbonne Universités, UPMC, Université Paris 06, CNRS, Laboratoire d'Océanographie de
15 Villefranche-sur-mer (LOV), 181 Chemin du Lazaret, 06230 Villefranche-sur-Mer, France

16 [4]Geotop, Université du Québec à Montréal, Montréal, Canada

17 [5]Aix Marseille Université, CNRS/INSU, Université de Toulon, IRD, Mediterranean Institute of
18 Oceanography (MIO) UM 110, 13288, Marseille, France

19

20

21

22

25

Abstract

26

27   Atmospheric input of anthropogenic lead increased globally over the last centuries. The

28 present study shows that the concentrations of lead in sediment cores from low-productivity

29 Hudson Bay, northern Canada, remained relatively constant over the last centuries. The lack of

30 imprint of the increased anthropogenic lead input in this marine environment is not consistent

31 with the increased lead concentrations in nearby lakes over the same period. In addition, the

32 observed trend in lead isotopic composition in our cores suggests an apparent progressive

33 overprint of anthropogenic lead during the 1900's. In other words, isotopes clearly registered the

34 increasingly anthropogenic nature of lead in the sedimentary record, but total lead concentrations

35 remained constant, indicating that some process limited the export of lead to the sediment. These

36 observations point to a long-term limitation of the downward export of particles in Hudson Bay.

37 Given that the source of lead was the same for both Hudson Bay and neighboring high-

38 productivity lakes, we hypothesize that the very low primary productivity of Hudson Bay waters

39 was responsible for the low vertical export of lead to marine sediments. We further propose that

40 primary productivity is the most important factor that generally drives the vertical export of

41 particulate matter, and thus hydrophobic contaminants, in near-oligotrophic marine environments.

42

43

1. Introduction

Atmospheric transportation of anthropogenic contaminants over thousands of kilometers was reported in the late 1970s as the main mechanism explaining the presence of contaminants at high latitude (Rahn et al. 1977; Barrie et al. 1981). However, the precise mechanisms by which insoluble contaminants deposited at the water surface are exported to depth are still not completely resolved. The settling velocity of individual atmospheric particles with a diameter <5 µm (e.g. dust, sea spray, volcanic ash, anthropogenic material (De Angelis and Gaudichet 1991)) is null or very low in seawater, based on Stokes's law (Buat-Ménard et al. 1989), and their removal from the surface ocean depends on their aggregation with larger particulate biogenic material. The adsorption/aggregation of lithogenic atmospheric material (mostly dust) on/with organic particles are likely to increase the density, and thus the settling velocity of the resulting aggregates (Deuser et al. 1983; Fowler et al. 1987; Alldredge and Silver 1988; Jackson and Burd 1998; Armstrong et al. 2002; Francois et al. 2002; Turner 2002; Burd and Jackson 2009). However, recent studies indicate that, even if this 'ballast effect' probably increases the settling velocity of the sinking material, it may not be the main determinant of the downward export flux (Passow 2004; Heimbürger et al. 2014).

Tight coupling between primary productivity and downward fluxes of particulate organic carbon (POC) has been observed in various marine regions (Gačić et al. 2002; Migon et al. 2002; Boyce et al. 2010; Passow and Carlson 2012; Yool et al. 2013; Turner 2015). This indicates that biological productivity can lead to efficient export of atmospheric material to the sediment by inclusion of biogenic material in mineral-organic aggregates. Given that phytoplankton dynamics is controlled by nutrient availability, the environmental conditions that control limiting nutrients ultimately control the downward export of POC (Lampitt et al. 2010; Heimbürger et al. 2013).

Climate in the Arctic and more generally at high latitudes underwent dramatic changes during the past decades (Macdonald et al. 2005). The 20th century was the warmest period in the Arctic in at least 44,000 years (Miller et al. 2013), and environmental changes included increases in precipitation and river discharge as well as declines in snow cover and sea-ice extent (ACIA 2004). While the effects of such changes on primary productivity could be variable over Arctic shelves (Michel et al. 2015), they may have important consequences on the rates of contaminant scavenging and export from surface to deep water. For example, Outridge et al. (2007) suggested

74 that the 20th century increase in the accumulation of Hg in the sediment of a Canadian high Arctic

75 lake had largely been driven by an increase in autochthonous primary productivity since 1854.

76   In the present study, we hypothesized that low primary productivity was the main forcing

77 factor that determined the sedimentation of atmospherically-deposited matter in Hudson Bay

78 during the last centuries. To test this hypothesis, we investigated the concentration and isotopic

79 signature of Pb in two sediment cores from Hudson Bay, and compared these values with already

80 published sedimentary records from nearby high-productivity lakes (Outridge et al. 2002). We

81 used Pb because its multiple isotopes allow the identification of sources. Moreover, the pollution

82 history of Pb is well documented, especially around Hudson Bay where Pb was measured in lake

83 sediments. Our hypothesis would be rejected if (1) the sedimentary accumulation of Pb during

84 the last century were the same in the sedimentary records of both low-productivity Hudson Bay

85 and high-productivity nearby lakes, thus indicating that primary productivity did not play a key

86 role in the vertical export of Pb, or (2) the recent isotopic composition of records from Hudson

87 Bay and surrounding lakes were not recording the same anthropogenic signal.
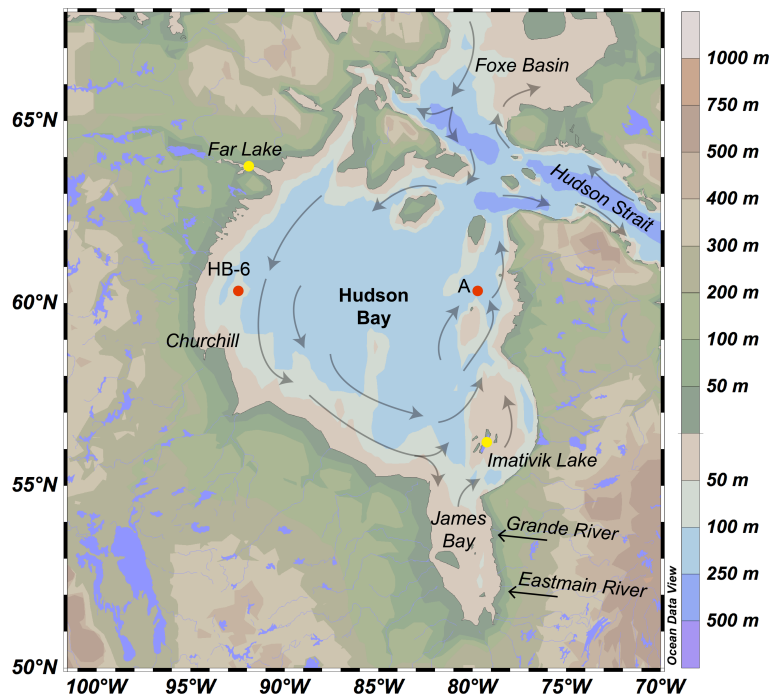
88

89 **2. Materials and Methods**

90 *2.1. Study area*

91   Hudson Bay has an area of about 841,000 km^2, an average depth of 125 m (maximum

92 depth of 250 m), and slopes generally less than 2 degrees (Prinsenberg 1986). Dense cold saline

93 water enters the Bay from the northwest (Hudson Strait and Foxe Basin, located in the north of

94 Hudson Bay; Fig. 1). Circulation inside the Bay is cyclonic, with surface currents averaging

95 5 cm s^{-1} in summer, and 2-3 cm s^{-1} in winter when the Bay is ice-covered (Saucier and Dionne

96 1998). There is a surface outflow of relatively warm and fresh water to the northeast of the Bay

97 towards Hudson Strait. Estimates of the residence time of surface (fresh) water are quite variable

98 in the literature, i.e. they range from the order of one month to more than 6 years (Prinsenberg

99 1984; Jones and Anderson 1994; Granskog et al. 2009). Many rivers discharge freshwater in the

100 southern part of Hudson Bay, causing a strong latitudinal surface salinity gradient. The annual

101 discharge (710 km^3 yr^{-1}) is equivalent to an annual freshwater yield of about 65 cm over the

102 whole bay (Prinsenberg 1986). This freshwater inflow has a profound influence on the physical,

103 chemical and biological properties of the Bay because it fosters stratification of the water column,

104 which usually reduces vertical mixing and thus upward transport of nutrients (Prinsenberg 1986).

105   Although the intense stratification may suggest that Hudson Bay is oligotrophic, a recent study
106   indicates that even if the riverine inputs are relatively minor sources of nitrate, the inputs of
107   freshwater favor rather than impede primary productivity inshore by indirectly fostering the
108   entrainment and upwelling of deeper water to the surface (Kuzyk et al. 2010a). Because Hudson
109   Bay is semi-enclosed within the Canadian Shield, its geochemical characteristics are strongly
110   influenced by local factors such as the geological substrates that are drained by river runoff, wet
111   and dry atmospheric depositions, and seasonal sea-ice formation and melt.

112

113

114   Fig. 1: Map of Hudson Bay with major currents. The two red dots indicate the locations of our two
115   sediment cores at about 60°N (Stations HB-6 and A), the yellow dots indicate the locations of the two
116   lakes to which our data are compared in the discussion and the two straight arrows on the eastern side of
117   James Bay represent major river inputs.

118

119   Despite its remote location, Hudson Bay is subject to anthropogenic contamination
120   through medium to long-range atmospheric transport, as is most of Northern Canada (Barrie et al.
121   1992; Outridge et al. 2002; Outridge et al. 2007; Kuzyk et al. 2010a; Outridge et al. 2011). The
122   different potential sources of anthropogenic lead contamination in the Arctic were traced using
123   lead isotopes, as each source is characterized by a specific isotopic signature linked essentially to

124   the mined ore deposits (Sturges and Barrie 1987; Sturges et al. 1993). The sources thus identified

125   were located in Canada, the USA, Europe and Russia (Sturges and Barrie 1987; Sturges and

126   Barrie 1989).

127

128   *2.2. Sediment cores*

129   The two sediment cores used for this study (Table 1) were chosen to capture the

130   characteristics of water masses that enter Hudson Bay (station HB-6), and those that are at the

131   end of the cyclonic gyre (station A). The two cores were collected using a box-corer during the

132   MERICA cruise (étude des MERs Intérieures du Canada) in summers 2003 (station A) and 2004

133   (station HB-6). The sediment cores were collected and provided to us by Michel Starr (Maurice

134   Lamontagne Institute, Fisheries and Oceans Canada). Cores were stored in a cold room at 4°C

135   until 2006, when sub-samples were dried, crushed and stored at room temperature in the

136   laboratory. Analyses reported in this paper were performed in 2007 and 2010. Due to the

137   respective geographic locations of the two coring stations, the allochtonous material that reached

138   stations HB-6 and A originated from the western and eastern coasts of the Bay, respectively. The

139   proportion of marine organic carbon in the surface sediment in the vicinity of cores A and HB-6

140   was 80 to 85% of the total organic carbon, respectively (Kuzyk et al. 2009), stressing the

141   importance of autochthonous organic matter in the total organic sediment load of the two areas.

142

Station	Lat. (°N)	Long. (°W)	Depth (m)	Core length (cm)
HB-6	60.94°	91.78°	120	24
A	60.17°	79.00°	130	30

143   Table 1: Characteristics of the two coring stations and cores.

144

145   *2.3. Chronostratigraphy*

146   The activity of ^{210}Pb of dried and ground sediment samples was obtained indirectly by

147   measuring the decay rate of its daughter isotope ^{210}Po ($t_{1/2}$ = 138.4 days; α = 5.30 MeV) by alpha

148   spectrometry. Measurements were carried out more than 2 years after sampling to ensure that

149   secular equilibrium was reached. A ^{209}Po spike was added to the samples to determine the

150   extraction efficiency. Polonium was extracted and purified by chemical treatments (reacted

151 sequentially with HCl, HNO$_3$, HF and H$_2$O$_2$) and deposited on a silver disk (Flynn 1968). The

152 ^{209}Po and ^{210}Po activities were measured with a silicon surface barrier α-spectrometer

153 (EGG&ORTEC type 576A).

154 Cesium-137 was measured on dried and ground sediment samples (1 cm^3) by γ-ray

155 spectrometry at 661.6 keV (γ-ray yield = 85 %) using a low-background high-purity Ge well

156 detector (Canberra). Standard sediment (IAEA-300) was used to calibrate the yield of the

157 detector. Uncertainties were estimated for counting errors following the protocol of Not et al.

158 (2008).

159 Sedimentation accumulation rates (SAR) were calculated using the radioactive decay

160 constant (λ = 0.03114 yr^{-1}) of ^{210}Pb and the slope of the linear regression of the logarithm of

161 excess ^{210}Pb (i.e. ^{210}Pb scavenged from the water column) following the constant flux and

162 constant sedimentation model (CFCS), previously described by Sanchez-Cabeza and Ruiz-

163 Fernández (2012). Excess ^{210}Pb was estimated from the ^{210}Pb activity (Fig 2; data in the online

164 supplement) minus the supported ^{210}Pb (i.e. the ^{210}Pb produced locally from ^{226}Ra disintegration)

165 over depth. The supported ^{210}Pb was estimated using the asymptotic value of ^{210}Pb data at the

166 bottom of the core. The linear regression for sedimentation rates was applied to the middle part of

167 the core to avoid potential modern disturbance by bioturbation in the upper part of the core. We

168 considered that the topmost part of the core corresponded to the present time, as no sediment had

169 been lost during sampling. For the bottom part of the core, where no excess ^{210}Pb was measured,

170 we assumed a constant sedimentation rate.

171

172 *2.4. Isotope geochemistry*

173 In a clean-room (class 100) environment, about 50 mg of dry sedimentary material were

174 dissolved in a Teflon bomb with a mixture of HF–HNO$_3$ (10:1 ratio) on a hot plate at 110°C for

175 48 h, and then evaporated to dryness with a drop of HBr to help conversion to PbBr$_2$. In order to

176 ensure high purity of the separated Pb, double-pass ion chromatography was performed on AG1-

177 X8 resin in dilute HBr medium to remove matrix elements, followed by elution of Pb phase in

178 6M HCl (similar to Manhes et al., 1978). The procedural blank value was negligible (i.e. average

179 value of 42 pg Pb for 1,250,000 pg Pb of sample). Mass spectrometry was done on an IsoProbe

180 multi-collector ICP-MS, with an Aridus desolvating membrane as the introduction system. A

181 transmission of 480 V/ppm was achieved using this set-up. All isotopes of Pb were measured on

182 Faraday detectors with 10^{11} Ω resistors, with amplifiers cross-calibrated in the morning during

183 the plasma warm-up time. Mass bias of samples was obtained using the NBS-991 Tl doping

184 technique (with a Pb/Tl = 10 to 12), and the correlation between Pb and Tl mass biases was

185 calculated from the repeated analysis of NBS-981 (Belshaw et al. 1998). Long-term

186 reproducibility of the internal standard was better than 0.03% on isotopic ratios normalized to

187 ^{204}Pb. The external analytical uncertainty on the isotopic ratios normalized to ^{204}Pb is on the third

188 digit (4th digit for the ^{206}Pb/^{207}Pb ratio). Any larger change in isotopic composition was thus

189 considered as significant.   All reagents used were distilled in sub-boiling stills, and subsequently

190 diluted with Milli-Q water.

191

192 *2.5. Lead and aluminium analysis*

193   Lead concentrations were measured on sediment core samples, and aluminum (Al)

194 concentrations were used to normalize Pb. Aluminum was considered to be a purely lithogenic

195 element representative of the input of the detrital component into the sediment. Indeed, very little

196 or no Al of anthropogenic origin is thought to reach the study region, as the Hudson Bay is

197 extremely remote and there is no significant industrial release of Al in these water. Moreover,

198 aluminum is commonly used to normalize various elements because its natural sources highly

199 exceed its anthropogenic sources (Daskalakis and O'Connor 1995; Heimbürger et al. 2012;

200 Heimbürger et al. 2014; St. Pierre et al. 2015). All reagents were certified Suprapur® and

201 provided by Merck (Darmstadt, Germany). All samples were handled under laminar airflow in a

202 class-100 clean room. Dry bulk sediments were ground using an agate mortar. Thirty milligrams

203 of ground sediment were weighted using a precision balance (Sartorius MC 1, accuracy 0.01 mg),

204 and transferred to a Teflon flask. The organic and carbonate matrices were destroyed as follows:

205 2 mL HCl 37% and 1 mL HNO_3 65% were added to the flask and heated at 130°C for 4 h. Next,

206 1 mL of HF 40% and 2 mL HNO_3 65% were added to the flask to dissolve the silicate material,

207 which was then heated at 130°C for 4 h or until complete evaporation. The residue was

208 ultrasonically dissolved in 1 mL HNO_3 1N, and made up to 9 mL with Milli-Q water. Trace

209 metal concentrations were measured using an Inductively Coupled Plasma Optical Emission

210 Spectrometer (SPECTRO ARCOS™) equipped with an autosampler (CETAC ASX-260™) and

211 an ultrasonic nebulizer (CETAC U5000AT™). Analytical procedures were validated using

212 international certified reference material (CRM) for sediment (NCS DC 75305 and IAEA-433),

213　aerosol (B3-0562). Replicates of CRM were always within the quoted confidence intervals

214　(values corresponding to "Certified" in Table 2). Detection limits (0.05 µg L^{-1} for Al, 0.01 µg L^{-1}

215　for Pb) were defined as three times the standard deviation of blank measurements for each metal,

216　and relative standard deviations were always <10% (results of the validation procedure are given

217　in Table 2). The anthropogenic enrichment of samples was estimated based on the Pb/Al ratio of

218　each sample divided by the Pb/Al ratio of the oldest samples in each core, which represent the

219　closest to natural background value available for our region. As Al indicates terrestrial input, this

220　index was used as a qualitative index of the sedimentary accumulation trend of non-terrestrial Pb.

221

	NCS-DC 75305 (µg g^{-1})	IAEA 433 (µg g^{-1})	B3-0562 (µg g^{-1})
Aluminium			
Measured (mean)	4.03 ± 0.297	80.39 ± 3.030	108.56 ± 1.37
Certified	4.08 ± 0.16	78.30 ± 4.30	107.91 ± 0.98
Lead			
Measured (mean)	22.2 ± 0.622	26.5 ± 0.329	16.94 ± 0.334
Certified	22.0 ± 1.1	26.0 ± 0.6	17.055 ± 0.195

222

223　Table 2: Certified reference material (CRM) validation results. Measurements were averaged

224　from 3 replicates.

225

226　**3. Results**

227　*3.1. Chronostratigraphy*

228　　　The chronology of all cores was based on ^{210}Pb (Fig. 2, blue curves). At station A, the

229　surface sample was lost, and the first sample was thus at 2 cm. The ^{210}Pb values decreased almost

230　linearly from 523 Bq g^{-1} at 2 cm to 88 Bq g^{-1} at 8 cm, after which they decreased slowly until

231　they reached the supported value of ~50 Bq g^{-1} at 27.5 cm. At station HB-6, ^{210}Pb was about

232　123 Bq g^{-1} at the surface of the core, and progressively increased to 176 Bq g^{-1} at 6 cm, after

233　which it decreased linearly to reach the supported value of ~73 Bq g^{-1} at 15 cm.

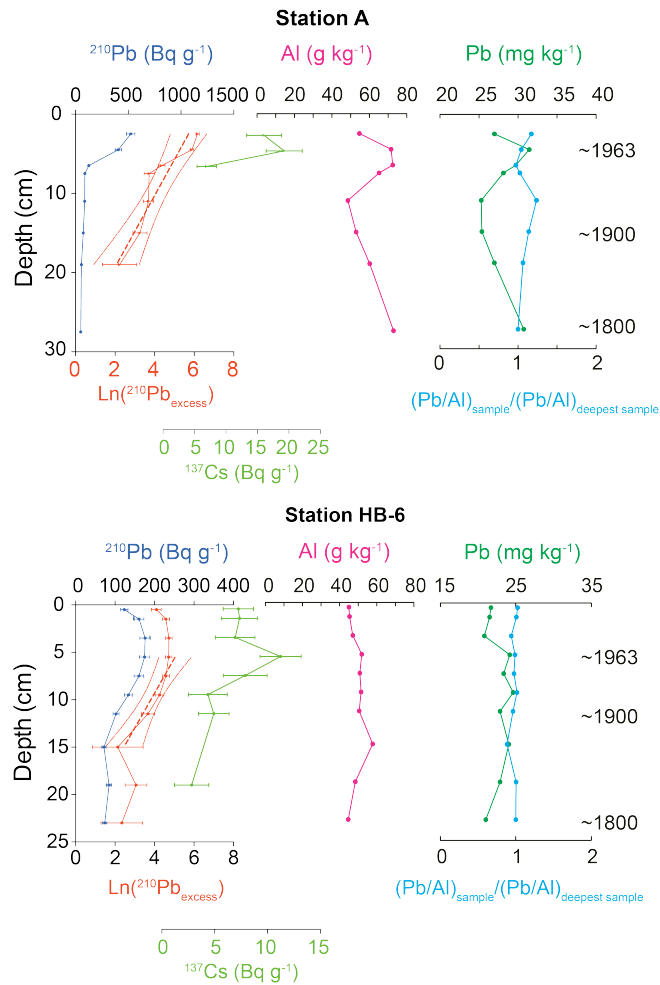234　　　We estimated the SAR using two approaches. Firstly, the CFCS model estimate yielded

235　sedimentation rates between 0.141 ± 0.032 cm yr^{-1} (r^2 = 0.86) and 0.114 ± 0.024 cm yr^{-1}

236   ($r^2 = 0.92$) for cores A and HB-6, respectively. Secondly, ^{137}Cs values peaked at 4.5 and 5.5 cm

237   for cores A and HB-6, respectively (Fig. 2). We calculated the SAR by dividing the depth of the

238   peak depth (4.5 and 5.5 cm) by the number of years between the time of sampling and 1963.

239   These ^{137}Cs-derived sedimentation rates were consistent with the CFCS-derived rate (0.113 and

240   0.134 cm yr^{-1} for cores A and HB-6 respectively).

241   We hypothesized that the sedimentation rate was constant over the whole period covered

242   by each core, and estimated the age of the sediment by dividing its depth in the core (cm) using

243   constant sedimentation rates of 0.094 to 0.141 and 0.115 to 0.192 cm yr^{-1} for cores HB-6 and A,

244   respectively. The estimated years corresponding to different depths in each core are indicated in

245   Fig. 2 (dashed horizontal lines, corresponding to the range of sedimentation rate estimates for

246   each core).

247   Our estimated sedimentation rates are based on the assumptions that the topmost part of

248   the cores corresponded to the present time, and we used a constant sedimentation rate for the

249   bottom part. Despite the resulting uncertainties, our estimates of 0.094 to 0.141 and 0.115 to

250   0.192 cm yr^{-1} for cores HB-6 and A, respectively are consistent with values previously estimated

251   for these marine areas of Hudson Bay, i.e. 0.05 to 0.17 cm yr^{-1} (Kuzyk et al. 2009; Hare et al.

252   2010). We also observed a ^{206}Pb/^{207}Pb profile shift from the natural background to anthropogenic

253   value in the 1800's, a sharper shift during the 1900's, and a strong dominance of anthropogenic

254   lead in the late 1900's (Fig. 3). However, because the resulting age estimates must be taken with

255   caution, we do not discuss here the precise timing of past events, but we examine instead the

256   general temporal trends of the lead concentrations and the isotope signature.
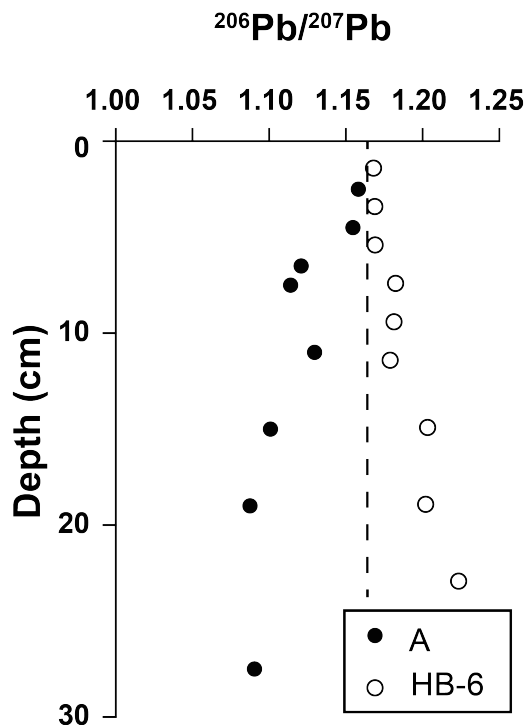
257

Fig. 2: Vertical profiles of ^{210}Pb, ^{137}Cs, Al and Pb in cores A (top) and HB-6 (bottom). Left panels. ^{210}Pb (Bq g^{-1}; blue, upper scale) and natural log of excess lead-210 (red, lower scale); different scales are used for the two stations. Red dashed lines: linear regressions of natural log of excess lead-210 on depth and their 95% confidence intervals. Middle panels. Profiles of Al (pink, mg kg^{-1}). Right panels. Pb concentration (green, mg kg^{-1}, upper scale), and enrichment ratio of Pb normalized to Al (blue, bottom scale). The dashed horizontal lines correspond to increasing age with depth (years are indicated), and the intervals indicate the uncertainties in our estimates. In the right panel, the enrichment ratio of Pb normalized to Al is provided on a 0-to-2 scale, where 1 indicates no enrichment compared to the oldest value recorded at the site, 2 represents a 2-time enrichment, and a value between 0 and 1 represents a decrease of Pb/Al compared to the oldest recorded value.

3.2. Lead geochemistry

Bottom-to-top variations in concentrations of Al and Pb were different in the two cores (Fig. 2, left and middle panels). At station A, Al and Pb increased by ~30% from 10 to 4 cm (i.e.
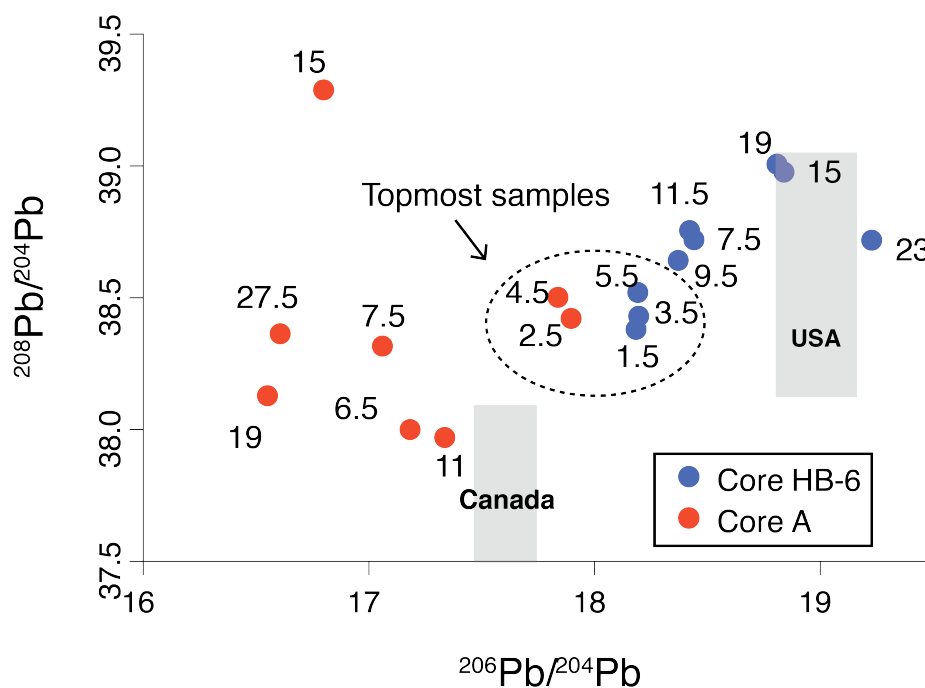
273   from the 1800's to the early 1900's), after which they both decreased in the topmost samples. At

274   station HB-6, there was no strong vertical variation in either the Al or Pb profile. In both cores,

275   variations in the enrichment ratio normalized to Al were small (Fig. 2, right panel). There was a

276   strong positive correlation between Pb and Al in the two cores (station A: $r = 0.95$, Prob <0.0005;

277   station HB-6: $r = 0.83$, Prob <0.005).

$$^{206}\text{Pb}/^{207}\text{Pb}$$

278

279

280   Fig. 3: $^{206}\text{Pb}/^{207}\text{Pb}$ ratio in cores HB-6 and A. The dashed vertical line represents the isotopic value of the

281   Arctic anthropogenic Pb (1.16; Sturges et al. 1993). The error bars are smaller than the dots (see text for

282   details).

283

284   Concerning the isotopes, there was a shift in $^{206}\text{Pb}/^{207}\text{Pb}$ in core A from 1.09 at the bottom

285   to about 1.16 in the topmost centimeters (Fig. 3). In core HB-6, the pattern was opposite, with the

286   bottom-to-top ratio shifting from 1.22 to 1.17. The isotopic values of the two cores converged at

287   the top. We also investigated the variations in ^{204}Pb, ^{206}Pb and ^{208}Pb as it had been suggested that

288   normalizing ^{206}Pb and ^{208}Pb to ^{204}Pb generally allows to distinguish between three mixed end-

289   members (Ellam 2010). In the scatter diagram of $^{208/204}\text{Pb}$ *vs* $^{206/204}\text{Pb}$ (Fig. 4; values in the

290   supplemental material), the ratios from the two cores are very far apart for the oldest samples and

291   progressively converge toward similar values for the most recent samples.

292

Fig. 4. Plot of the isotopic ratios $^{208/204}$Pb on $^{206/204}$Pb, along with national aerosol averaged values for two different potential source regions (grey boxes), i.e. Canada and the USA in the 1980's (Sturges and Barrie 1987; Graney et al. 1995; Poirier 2006). Each sample is labelled with its depth (in cm) in its core to highlight the temporal convergence of the isotope ratios from the two cores toward the same values.

4. Discussion

4.1. Historical variations in the sources of Pb

The Hudson Bay is characterized by intense sediment resuspension due to postglacial isostatic rebound (Hare et al. 2008; Kuzyk et al. 2009), which can dilute anthropogenic inputs in surface sediments (Hare et al. 2010). This could partly mask the sedimentary record of anthropogenic Pb, and thus prevent the use of our sediment records to investigate the vertical export of Pb during the last centuries. However, our cores clearly recorded Pb of anthropogenic origin, as shown by the convergent trend toward the anthropogenic value of 1.16 (Sturges and Barrie 1987) in Figure 3, and are thus suitable for investigating the vertical export dynamics of anthropogenic Pb as shown by the ^{210}Pb chronology, which was corroborated by a secondary stratigraphic marker (^{137}Cs).

Because Al in sediments traces the terrestrial inputs, the correlation between Pb and Al provides information on the importance of lithogenic inputs in the accumulation of Pb (Brumsack

13

312 2006). The strong positive correlations of Pb and Al in the two cores (Section 3.2) indicate that
313 the historical Pb accumulation was strongly controlled by terrestrial inputs. In addition, the
314 vertical export of terrestrial or atmospheric Pb from surface waters to the sediment would have
315 different effects on Pb concentration normalized to Al, i.e. terrestrial Pb would be deposited
316 together with terrestrial Al, hence constant Pb normalized to Al, whereas atmospheric Pb would
317 not be deposited together with terrestrial Al, hence higher Pb normalized to Al (Daskalakis and
318 O'Connor 1995; Heimbürger et al. 2012; Heimbürger et al. 2014). Moreover, enrichment factors
319 of mercury relative to aluminium have been similarly used to identify the source of mercury
320 (atmosphere against underlying soils) by St. Pierre et al. (2015). At our two stations, there were
321 no strong variations in the enrichment ratio of Pb normalized to Al along the cores, indicating
322 that the sedimentary accumulation of airborne Pb remained constant during the last 200 years in
323 the two cores.

324   Irrespective of the isotope considered, the two cores were characterized by a trend
325 (i.e. older to recent) that converged toward a value half way between typical historical Canadian
326 and USA lead emissions (Figs. 3 and 4). The oldest samples in the two cores were characterized
327 by opposite $^{206}Pb/^{207}Pb$, $^{206}Pb/^{204}Pb$ and $^{208}Pb/^{204}Pb$ isotopic signatures (Figs. 3 and 4), meaning
328 that early-industrial Pb inputs (i.e. between 1800 and 1900) originated from different sources in
329 the western and eastern parts of Hudson Bay. The temporal trends of $^{206}Pb/^{204}Pb$ and $^{208}Pb/^{204}Pb$
330 in core HB-6 are similar to those observed in two Hudson Bay lakes (Outridge et al. 2002),
331 suggesting similar early-industrial sources of lead on the western side of the Bay. The early-
332 industrial $^{206}Pb/^{207}Pb$ isotopic signature was different in cores A and HB-6 (1.10 and 1.22,
333 respectively), on the eastern and western sides of the Bay, respectively. This probably reflected
334 the spatial heterogeneity that exists in the different potential sources of Pb (with different isotopic
335 signatures) in the Canadian shield, which surrounds most of Hudson Bay (GEOROC 2003). The
336 isotopic ratio values toward which the two cores converged were the same as in surrounding
337 lakes on the two sides of Hudson Bay (Fig. 3 in this study, and Figs. 6 and 7 in Outridge et al.
338 2002). Irrespective of the early-industrial sources, the fact that the isotopic composition in the
339 two cores started with different values and converged toward a single value indicates that both
340 cores recorded the imprint of medium to long-range anthropogenic Pb deposition during the last
341 century.

342

343   *4.2. Effect of primary productivity on the sedimentary Pb record*

344   Local anthropogenic inputs of metals are low in the Hudson Bay area because of its

345   remote location and the scarcity of industries. Hence, medium to long-range atmospheric

346   transport was presumably the main source of anthropogenic contaminants. A small increase from

347   25 to 30 mg kg^{-1} in Pb concentration was observed in sediment core A around 6 and 7 cm (Fig. 2).

348   However, because a similar increase was also observed in Al, Pb normalized to Al was mostly

349   constant, which suggested that Pb was of terrestrial origin. This is consistent with the slight

350   reduction in ^{206}Pb/^{207}Pb near 6 and 7 cm in core A indicating a transient return to more terrestrial

351   (background) values. This transient increase in terrestrial input could be related to increased

352   precipitation due to the climatic variability of Hudson Bay (Guiot 1987). In core HB-6, the record

353   showed no sign of increase in either Pb concentration or Pb/Al, suggesting relatively constant Pb

354   input (terrestrial and atmospheric) during the last two centuries in this part of the bay. The ~20%

355   increase in Pb concentration in core A is much smaller than the three- to five-fold increase in Pb

356   concentration in the recent sediments (last century) of two lakes in the Hudson Bay (Outridge et

357   al. 2002). The observed increase in Pb in lake sediments was attributed by Outridge et al. (2002)

358   to medium to long-range atmospheric inputs of anthropogenic Pb originating from Eurasia and

359   North America. Because waters of the lakes and Hudson Bay should have been both exposed to

360   similar inputs of atmospheric materials, the difference in Pb accumulation between the two

361   environments indicates that the transfer mechanisms of Pb to the sediment where different in the

362   two environments, assuming no diagenetic or post-sampling effect on Pb concentrations. The

363   ^{206}Pb/^{207}Pb isotopic values (Fig. 3) show, for the cores on the two sides of the Hudson Bay, an

364   apparent progressive overprint of anthropogenic lead (from bottom to top of cores) during the

365   1900's, whose isotopic ratio reflects a mixed Canada-USA aerosol origin (^{206}Pb/^{207}Pb = 1.16-

366   1.17; Sturges and Barrie 1987). In other words, despite a globally increased atmospheric import

367   of anthropogenic lead (Nriagu 1996), the amount of Pb deposited in Hudson Bay's sediment did

368   not change dramatically during the last century, but the sources of emission changed as shown by

369   changes in the isotope ratios. This indicates that sedimentary accumulation of anthropogenic Pb

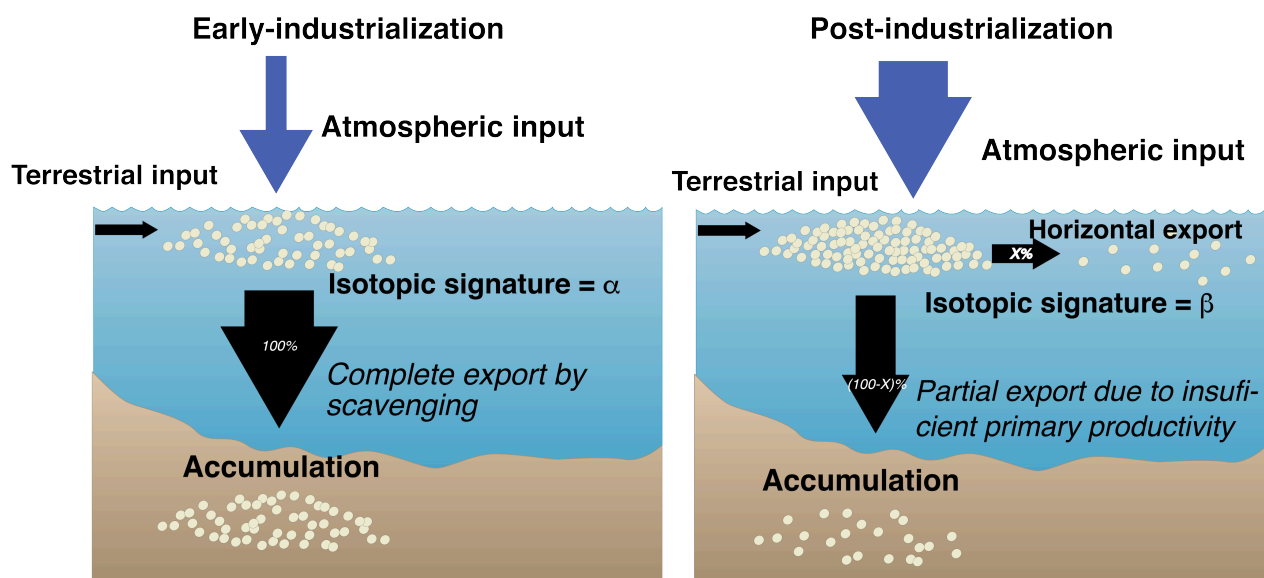370   was limited in Hudson Bay by a factor that acted differently in the bay than in surrounding lakes.

371   Assuming a typical sinking velocity of 20 to 200 m d^{-1} for Pb when packaged within

372   biogenic aggregates (Alldredge and Gotschalk 1988; Armstrong et al. 2009; McDonnell and

373   Buesseler 2010), i.e. when sedimentation is driven by biological productivity, surface Pb would

374 reach 250 m (i.e. the maximum depth of Hudson Bay) within less than 15 days (the depths of

375 coring sites HB-6 and A were 120 and 130 m, respectively). Hence even if the estimates of the

376 residence time of Hudson surface waters vary over a wide range in the literature (i.e. from one

377 month to 6 years, Section 2.1), Pb packaged within biogenic aggregates should sediment within

378 the Bay. As a result, the only ways by which Pb would have not reached the sediment should

379 have been either a lack of aggregation due to very low biological productivity, and/or a very low

380 sinking velocity of the Pb-containing aggregates, i.e. $\ll 20$ m d^{-1}. These two conditions would

381 have led Pb to be flushed out of the bay.

382 Our results and previously published data show that the sedimentary accumulation of Pb

383 in the last century was not the same in the records of low-productivity Hudson Bay as in the high-

384 productivity nearby lakes, whereas the recent isotopic composition was the same in sediments

385 from both Hudson Bay and the surrounding lakes (Outridge et al. 2002). Hence, we cannot reject

386 our initial hypothesis that primary productivity was the main forcing factor determining the

387 sedimentation of airborne matter. This hypothesis is consistent with the suggestion from previous

388 studies that sedimentary sequences in Hudson Bay did not always record directly the atmospheric

389 deposition of allochthonous matter, but could be affected by low primary productivity. For

390 example and similarly to our Pb observations, it was recently suggested that the sedimentation of

391 polychlorinated biphenyl (PCBs) was exceptionally low in Hudson Bay, because the very low

392 productivity in the Bay and the resulting weak downward flux of organic matter inhibited the

393 transfer of PCBs from surface to depth and, therefore, their sedimentation (Kuzyk et al. 2010a).

394 Such a relationship between primary productivity and the downward flux of aggregates may be a

395 typical feature of many environments in the world ocean (Passow 2004; Heimbürger et al. 2014).

396 The conceptual model in Fig. 5 summarizes the above ideas, illustrating the early-

397 industrial and post-industrial situations in Hudson Bay. In the early-industrial model, atmospheric

398 inputs of Pb were low, and this Pb was characterized by the local isotopic signature α. Most Pb,

399 perhaps all, was exported downwards and accumulated in the sediment after being scavenged by

400 organic particles, thus transferring the isotopic signature of Pb from surface waters to the

401 sediment. The post-industrialization model is characterized by a higher rate of Pb input from the

402 atmosphere to the surface water due to the enhanced medium to long-range transport of

403 anthropogenic Pb (Outridge et al. 2002). This Pb is characterized by the different isotopic

404 signature β, which reflects its mixed local and anthropogenic origins. The similar concentration

405 of Pb accumulated in the sediment is explained by a limitation of its export by the low primary
406 productivity of Hudson Bay, which restricts the availability of organic particles to scavenge Pb
407 and export it to the sediment. As a consequence, despite a likely increase in atmospheric
408 deposition of Pb with increased industrialization, its accumulation was similar after and before
409 industrialization, but its isotopic signature was different in the two periods.

410

Early-industrialization

Atmospheric input

Terrestrial input

Isotopic signature = α

100%

Complete export by scavenging

Accumulation

Post-industrialization

Atmospheric input

Terrestrial input

Horizontal export

X%

Isotopic signature = β

(100-X)%

Partial export due to insufi-cient primary productivity

Accumulation

411

412 Fig. 5. Schematic representation of our hypothesis on the atmospheric and water-column fluxes of
413 contaminants before and after industrialization in Hudson Bay. The illustrated mechanisms explain both
414 the absence of difference in Pb sedimentary accumulation, and the change in the isotopic signatures of
415 sediments from the early-industrial to the post-industrial period.

416

417   Enhanced atmospheric inputs of contaminants in the last century were not significantly
418 recorded in Hudson Bay sediments, presumably because of the exceptionally low productivity of
419 the Bay (Kuzyk et al. 2009), which prevented the efficient transfer of chemical elements from the
420 water column to the sediment. However, the signature of the Pb isotopes suggests a shift from
421 local input to medium to long-range anthropogenic inputs during the 20th century, which thus
422 recorded the signature of the last century. This is consistent with our hypothesis that low primary
423 productivity was the main forcing factor that determined the sedimentation of atmospherically-
424 deposited matter in Hudson Bay during the last century. This observation is globally significant
425 as Hudson Bay is extremely sensitive to warming, with an increase of 0.47°C per decade over the
426 last 50 years (Mulder et al. 2016). Warming will lead to increased river discharge, which could

427 enhance primary productivity in the Hudson Bay because river discharge promotes the upwelling

428 of deep waters (Kuzyk et al. 2010a; Kuzyk et al. 2010b). If Arctic regions are currently warming

429 up, one may expect increasing fluxes of nutrients to Hudson Bay, in the northern part of Canada.

430 It may therefore also be expected that the magnitude of primary productivity in Hudson Bay will

431 increase as well, which would lead to an increase in export fluxes of atmospherically-deposited

432 contaminants, once packaged with particulate biogenic matter.

433

434 *4.3. Possible effect of transparent exopolymer particles (TEP)*

435   It was mentioned above that one of the possible explanations to our observations was that

436 the Pb-containing aggregates sank at very low velocity. This could have occurred if the

437 aggregates formed in Hudson Bay had been neutrally buoyant, and had thus remained in surface

438 waters long enough to be flushed out of the Bay. While there are multiple factors that can

439 influence the particle settling velocity (Maggi 2013), the accumulation of positively buoyant

440 transparent exopolymer particles (TEP) in oligotrophic surface waters is hypothesized to

441 contribute to slowing down the downward export flux (Azetsu-Scott and Passow 2004, Mari et al.

442 2017).

443   The increase of TEP volume concentration in surface waters is a significant feature in

444 some oligotrophic waters, e.g. the Mediterranean Sea (Mari et al. 2001; Bar-Zeev et al. 2011), the

445 Pacific Ocean (Wurl et al. 2011; Kodama et al. 2014), and Hudson Bay (Michel et al. 2006). The

446 limited TEP dataset for Hudson Bay is characterized by a sub-surface maximum around 50 m

447 where it co-occurs with the chlorophyll *a* maximum, suggesting a link between the two (Michel

448 et al. 2006). Nutrient limitation increases the production of TEP by phytoplankton and lowers

449 their bacterial degradation, and the two processes contribute to TEP accumulation in surface

450 waters (Mari et al. 2001, 2017). Owing to their high stickiness, TEP are often seen as a catalyst of

451 aggregation, and thus a key component for the formation of fast-sinking aggregates (Passow et al.

452 2001), but (Mari et al. 2017) proposed that a system with high volume concentration of low-

453 density TEP and low concentration of dense particles in surface waters should be characterized

454 by low downward POC export (Mari et al. 2017). The latter conditions are those observed during

455 periods of severe oligotrophy in Hudson Bay, where the accumulation of TEP in surface waters

456 could have enhanced the residence time of TEP-associated elements (e.g. Pb) and particles

457 (e.g. mineral dust) in surface, thus favoring their horizontal export out of the bay instead of
458 downward export.
459

460 **Acknowledgements**

References

ACIA (2004) Impacts of a Warming Arctic: Arctic Climate Impact Assessment. ACIA Overv. Rep. 140.

Alldredge AL, Gotschalk C (1988) In situ settling behavior of marine snow. Limnol Oceanogr 33:339–35. doi: 10.4319/lo.1988.33.3.0339

Alldredge AL, Silver MW (1988) Characteristics, dynamics and significance of marine snow. Prog Oceanogr 20:41–82. doi: 10.1016/0079-6611(88)90053-5

Armstrong RA, Lee C, Hedges JI, et al (2002) A new, mechanistic model for organic carbon fluxes in the ocean based on the quantitative association of POC with ballast minerals. 49:219–236. doi: 10.1016/S0967-0645(01)00101-1

Armstrong RA, Peterson ML, Lee C, Wakeham SG (2009) Settling velocity spectra and the ballast ratio hypothesis. Deep Res Part II Top Stud Oceanogr 56:1470–1478. doi: 10.1016/j.dsr2.2008.11.032

Azetsu-Scott K, Passow U (2004) Ascending marine particles: Significance of transparent exopolymer particles (TEP) in the upper ocean. Limnol Oceanogr 49:741–748. doi: 10.4319/lo.2004.49.3.0741

Bar-Zeev E, Berman T, Rahav E, et al (2011) Transparent exopolymer particle (TEP) dynamics in the eastern Mediterranean Sea. Mar Ecol Prog Ser 431:107–118. doi: 10.3354/meps09110

Barrie LA, Gregor D, Hargrave B, et al (1992) Arctic contaminants: sources, occurrence and pathways. Sci Total Environ 122:1–74. doi: 10.1016/0048-9697(92)90245-N

Barrie LA, Hoff RM, Daggupaty SM (1981) The influence of mid-latitudinal pollution sources on haze in the Canadian arctic. Atmos Environ 15:1407–1419. doi: 10.1016/0004-6981(81)90347-4

Belshaw N, Freedman P, O'Nions R, et al (1998) A new variable dispersion double-focusing plasma mass spectrometer with performance illustrated for Pb isotopes. Int J Mass Spectrom 181:51–58. doi: 10.1016/S1387-3806(98)14150-7

Boyce DG, Lewis MR, Worm B (2010) Global phytoplankton decline over the past century. Nature 466:591–596. doi: 10.1038/nature09268

Brumsack HJ (2006) The trace metal content of recent organic carbon-rich sediments: Implications for Cretaceous black shale formation. Palaeogeogr Palaeoclimatol Palaeoecol 232:344–361. doi: 10.1016/j.palaeo.2005.05.011

Buat-Ménard P, Davies J, Remoudaki E, et al (1989) Non-steady-state biological removal of atmospheric particles from Mediterranean surface waters. Nature 340:131–134. doi: 10.1038/340131a0

Burd AB, Jackson GA (2009) Particle aggregation. Ann Rev Mar Sci 1:65–90. doi: 10.1146/annurev.marine.010908.163904

Daskalakis KD, O'Connor TP (1995) Normalization and elemental sediment contamination in the coastal United States. Environ Sci Technol 29:470–477. doi: 10.1021/es00002a024

De Angelis M, Gaudichet A (1991) Saharan dust deposition over Mont Blanc (French Alps) during the last 30 years. Tellus 43B:61–75. doi: 10.1034/j.1600-0889.1991.00005.x

Deuser WG, Brewer PG, Jickells TD, Commeau RF (1983) Biological control of the removal of abiogenic particles from the surface ocean. Science (80-) 219:388–391. doi: 10.1126/science.219.4583.388

Ellam RM (2010) The graphical presentation of lead isotope data for environmental source apportionment. Sci Total Environ 408:3490–3492. doi: 10.1016/j.scitotenv.2010.03.037

Flynn WW (1968) The determination of low levels of polonium-210 in environmental materials. Anal Chim Acta 43:221–227. doi: 10.1016/S0003-2670(00)89210-7

Fowler SW, Buat-Ménard P, Yokoyama Y, et al (1987) Rapid removal of Chernobyl fallout from Mediterranean surface waters by biological activity. Nature 329:56–58. doi: 10.1038/329056a0

Francois R, Honjo S, Krishfield R, Manganini S (2002) Factors controlling the flux of organic carbon to the bathypelagic zone of the ocean. Global Biogeochem Cycles 16:1087. doi: 10.1029/2001gb001722

Gačić M, Civitarese G, Miserocchi S, et al (2002) The open-ocean convection in the Southern Adriatic: A controlling mechanism of the spring phytoplankton bloom. Cont Shelf Res 22:1897–1908. doi: 10.1016/S0278-4343(02)00050-X

GEOROC (2003) Geochemistry of Rocks of the Oceans and Continents. In: MPI für Chemie/Max-Planck Inst. für Chemie, Mainz, Ger.

Graney JR, Halliday AN, Keeler GJ, et al (1995) Isotopic record of lead pollution in lake sediments from the northeastern United States. Geochim Cosmochim Acta 59:1715–1728. doi: 10.1016/0016-7037(95)00077-D

Granskog MA, Macdonald RW, Kuzyk ZZA, et al (2009) Coastal conduit in southwestern Hudson Bay (Canada) in summer: Rapid transit of freshwater and significant loss of colored dissolved organic matter. J Geophys Res Ocean 114:C08012. doi: 10.1029/2009JC005270.

524 Guiot J (1987) Reconstruction of seasonal temperatures in Central Canada since A.D. 1700 and detection of the 18.6-
525   and 22-year signals. Clim Change 10:249–268. doi: 10.1007/BF00143905
526 Hare AA, Stern GA, Kuzyk ZZA, et al (2010) Natural and anthropogenic mercury distribution in marine sediments
527   from Hudson Bay, Canada. Environ Sci Technol 44:5805–5811. doi: 10.1021/es100724y
528 Hare A, Stern GA, Macdonald RW, et al (2008) Contemporary and preindustrial mass budgets of mercury in the
529   Hudson Bay Marine System: The role of sediment recycling. Sci Total Environ 406:190–204. doi:
530   10.1016/j.scitotenv.2008.07.033
531 Heimbürger L-E, Cossa D, Thibodeau B, et al (2012) Natural and anthropogenic trace metals in sediments of the
532   Ligurian Sea (Northwestern Mediterranean). Chem Geol 291:141–151. doi: 10.1016/j.chemgeo.2011.10.011
533 Heimbürger LE, Lavigne H, Migon C, et al (2013) Temporal variability of vertical export flux at the DYFAMED
534   time-series station (Northwestern Mediterranean Sea). Prog Oceanogr 119:59–67. doi:
535   10.1016/j.pocean.2013.08.005
536 Heimbürger LE, Migon C, Losno R, et al (2014) Vertical export flux of metals in the Mediterranean Sea. Deep Res
537   Part I Oceanogr Res Pap 87:14–23. doi: 10.1016/j.dsr.2014.02.001
538 Jackson GA, Burd AB (1998) Aggregation in the marine environment. Environ Sci Technol 32:2805–2814. doi:
539   10.1021/es980251w
540 Jones EP, Anderson LG (1994) Northern Hudson Bay and Foxe Basin: Water masses, circulation and productivity.
541   Atmosphere-Ocean 32:361–374. doi: 10.1080/07055900.1994.9649502
542 Kodama T, Kurogi H, Okazaki M, et al (2014) Vertical distribution of transparent exopolymer particle (TEP)
543   concentration in the oligotrophic western tropical North Pacific. Mar Ecol Prog Ser 513:29–37. doi:
544   10.3354/meps10954
545 Kuzyk ZZA, Macdonald RW, Johannessen SC, et al (2009) Towards a sediment and organic carbon budget for
546   Hudson Bay. Mar Geol 264:190–208. doi: 10.1016/j.margeo.2009.05.006
547 Kuzyk ZZA, MacDonald RW, Johannessen SC, Stern GA (2010a) Biogeochemical controls on PCB deposition in
548   Hudson Bay. Environ Sci Technol 44:3280–3285. doi: 10.1021/es903832t
549 Kuzyk ZZA, Macdonald RW, Tremblay JÉ, Stern GA (2010b) Elemental and stable isotopic constraints on river
550   influence and patterns of nitrogen cycling and biological productivity in Hudson Bay. Cont Shelf Res 30:163–
551   176. doi: 10.1016/j.csr.2009.10.014
552 Lampitt RS, Salter I, de Cuevas BA, et al (2010) Long-term variability of downward particle flux in the deep
553   northeast Atlantic: Causes and trends. Deep Res Part II Top Stud Oceanogr 57:1346–1361. doi:
554   10.1016/j.dsr2.2010.01.011
555 Macdonald RW, Harner T, Fyfe J (2005) Recent climate change in the Arctic and its impact on contaminant
556   pathways and interpretation of temporal trend data. Sci. Total Environ. 342:5–86.
557 Maggi F (2013) The settling velocity of mineral, biomineral, and biological particles and aggregates in water. J
558   Geophys Res Ocean 118:2118–2132. doi: 10.1002/jgrc.20086
559 Manhes G, Minster JF, Allègre CJ (1978) Comparative uranium-thorium-lead and rubidium-strontium study of the
560   Saint Sèverin amphoterite: consequences for early solar system chronology. Earth Planet Sci Lett 39:14–24.
561   doi: 10.1016/0012-821X(78)90137-1
562 Mari X, Beauvais S, Lemée R, Pedrotti ML (2001) Non-Redfield C:N ratio of transparent exopolymeric particles in
563   the northwestern Mediterranean Sea. Limnol Oceanogr 46:1831–1836. doi: 10.4319/lo.2001.46.7.1831
564 Mari X, Passow U, Migon C, et al (2017) Transparent exopolymer particles: Effects on carbon cycling in the ocean.
565   Prog Oceanogr 151:13–37. doi: http://dx.doi.org/10.1016/j.pocean.2016.11.002
566 McDonnell AMP, Buesseler KO (2010) Variability in the average sinking velocity of marine particles. Limnol
567   Oceanogr 55:2085–2096. doi: 10.4319/lo.2010.55.5.2085
568 Michel C, Hamilton J, Hansen E, et al (2015) Arctic Ocean outflow shelves in the changing Arctic: A review and
569   perspectives. Prog Oceanogr 139:66–88. doi: 10.1016/j.pocean.2015.08.007
570 Michel C, Lapoussiere A, LeBlanc B, Starr M (2006) Transparent expopolymeric substances (TEP) in Hudson Bay
571   during fall: significance and potential roles. http://www.arcticnet.ulaval.ca/pdf/posters_2006/michel_eT_al.pdf.
572   Accessed 22 Aug 2016
573 Migon C, Sandroni V, Marty JC, et al (2002) Transfer of atmospheric matter through the euphotic layer in the
574   northwestern Mediterranean: Seasonal pattern and driving forces. Deep Res Part II Top Stud Oceanogr
575   49:2125–2141. doi: 10.1016/S0967-0645(02)00031-0
576 Miller GH, Lehman SJ, Refsnider KA, et al (2013) Unprecedented recent summer warmth in Arctic Canada.
577   Geophys Res Lett 40:5745–5751. doi: 10.1002/2013GL057188
578 Mulder CPH, Iles DT, Rockwell RF (2016) Increased variance in temperature and lag effects alter phenological
579   responses to rapid warming in a subarctic plant community. Glob. Chang. Biol.

580 Not C, Hillaire-Marcel C, Ghaleb B, et al (2008) 210 Pb– 226 Ra– 230 Th systematics in very low sedimentation rate
581   sediments from the Mendeleev Ridge (Arctic Ocean). Can J Earth Sci 45:1207–1219. doi: 10.1139/E08-047
582 Nriagu JO (1996) A History of Global Metal Pollution. Science (80-) 272:223–0. doi: 10.1126/science.272.5259.223
583 Outridge P., Hermanson M., Lockhart W. (2002) Regional variations in atmospheric deposition and sources of
584   anthropogenic lead in lake sediments across the Canadian Arctic. Geochim Cosmochim Acta 66:3521–3531.
585   doi: 10.1016/S0016-7037(02)00955-9
586 Outridge PM, Rausch N, Percival JB, et al (2011) Comparison of mercury and zinc profiles in peat and lake sediment
587   archives with historical changes in emissions from the Flin Flon metal smelter, Manitoba, Canada. Sci Total
588   Environ 409:548–563. doi: 10.1016/j.scitotenv.2010.10.041
589 Outridge PM, Sanei LH, Stern G a, et al (2007) Evidence for control of mercury accumulation rates in Canadian
590   High Arctic lake sediments by variations of aquatic primary productivity. Environ Sci Technol 41:5259–65.
591 Passow U (2004) Switching perspectives: Do mineral fluxes determine particulate organic carbon fluxes or vice
592   versa? Geochemistry Geophys Geosystems 5:1–5. doi: 10.1029/2003GC000670
593 Passow U, Carlson CA (2012) The biological pump in a high CO_2 world. Mar Ecol Prog Ser 470:249–271. doi:
594   10.3354/meps09985
595 Passow U, Shipe RF, Murray A, et al (2001) The origin of transparent exopolymer particles (TEP) and their role in
596   the sedimentation of particulate matter. Cont Shelf Res 21:327–346. doi: 10.1016/S0278-4343(00)00101-1
597 Poirier A (2006) Re-Os and Pb isotope systematics in reduced fjord sediments from Saanich Inlet (Western Canada).
598   Earth Planet Sci Lett 249:119–131. doi: 10.1016/j.epsl.2006.06.048
599 Prinsenberg SJ (1984) Freshwater contents and heat budgets of James Bay and Hudson Bay. Cont Shelf Res 3:191–
600   200. doi: 10.1016/0278-4343(84)90007-4
601 Prinsenberg SJ (1986) Chapter 10 The Circulation Pattern and Current Structure of Hudson Bay. In: Martini I (ed)
602   Canadian Inland seas: Elsevier Oceanography Series. Elsevier B.V., Amsterdam, The Netherlands, pp 187–204
603 Rahn KA, Borys RD, Shaw GE (1977) The Asian source of Arctic haze bands. Nature 268:713–715. doi:
604   10.1038/268713a0
605 Sanchez-Cabeza JA, Ruiz-Fernández AC (2012) 210Pb sediment radiochronology: An integrated formulation and
606   classification of dating models. Geochim Cosmochim Acta 82:183–200. doi: 10.1016/j.gca.2010.12.024
607 Saucier FJ, Dionne J (1998) A 3-D coupled ice-ocean model applied to Hudson Bay, Canada: The seasonal cycle and
608   time-dependent climate response to atmospheric forcing and runoff. J Geophys Res Ocean 103:27689–27705.
609   doi: 10.1029/98JC02066
610 St. Pierre KA, St. Louis VL, Kirk JL, et al (2015) Importance of Open Marine Waters to the Enrichment of Total
611   Mercury and Monomethylmercury in Lichens in the Canadian High Arctic. Environ Sci Technol 49:5930–
612   5938. doi: 10.1021/acs.est.5b00347
613 Sturges WT, Barrie LA (1989) Stable lead isotope ratios in arctic aerosols: evidence for the origin of arctic air
614   pollution. Atmos Environ 23:2513–2519. doi: 10.1016/0004-6981(89)90263-1
615 Sturges WT, Barrie LA (1987) Lead 206/207 isotope ratios in the atmosphere of North America as tracers of US and
616   Canadian emissions. Nature 329:144–146.
617 Sturges WT, Hopper JF, Barrie LA, Schnell RC (1993) Arctic air, snow and ice chemistryStable lead isotope ratios
618   in Alaskan arctic aerosols. Atmos Environ Part A Gen Top 27:2865–2871. doi: http://dx.doi.org/10.1016/0960-
619   1686(93)90317-R
620 Turner JT (2002) Zooplankton fecal pellets, marine snow and sinking phytoplankton blooms. Aquat Microb Ecol
621   27:57–102. doi: 10.3354/ame027057
622 Turner JT (2015) Zooplankton fecal pellets, marine snow, phytodetritus and the ocean's biological pump. Prog
623   Oceanogr 130:205–248. doi: 10.1016/j.pocean.2014.08.005
624 Wurl O, Miller L, Vagle S (2011) Production and fate of transparent exopolymer particles in the ocean. J Geophys
625   Res Ocean 116:C00H13. doi: 10.1029/2011JC007342
626 Yool A, Popova EE, Coward AC, et al (2013) Climate change and ocean acidification impacts on lower trophic
627   levels and the export of organic carbon to the deep ocean. Biogeosciences 10:5831–5854. doi: 10.5194/bg-10-
628   5831-2013
629